# Single-vesicle measurement of protein-induced membrane tethering

Bin Cai[a,b], Luning Yu[c], Savanna R. Sharum[d], Kai Zhang[d,*], Jiajie Diao[a,*]

[a] Department of Cancer Biology, University of Cincinnati, Cincinnati, OH 45267, USA
[b] Research Center for Nano-Biomaterial, Analytical & Testing Center, Sichuan University, Chengdu 610064, China
[c] Department of Physics, University of Cincinnati, Cincinnati, OH 45221, USA
[d] Department of Biochemistry, University of Illinois at Urbana-Champaign, Urbana, IL 61801, USA

A B S T R A C T

Functions of the proteins involved in membrane tethering, a crucial step in membrane trafficking, remain elusive due to the lack of effective tools to investigate protein-lipid interaction. To address this challenge, we introduce a method to study protein-induced membrane tethering via in vitro reconstitution of lipid vesicles, including detailed steps from the preparation of the PEGylated slides to the imaging of single vesicles. Furthermore, we demonstrate the measurement of protein-vesicle interaction in tethered vesicle pairs using two representative proteins, the cytoplasmic domain of synaptotagmin-1 (C2AB) and α-synuclein. Results from Förster (fluorescence) resonance energy transfer (FRET) reveal that membrane tethering is distinguished from membrane fusion. Single-vesicle measurement also allows for assessment of dose-dependent effects of proteins and ions on membrane tethering. We envision that the continuous development of advanced techniques in the single-vesicle measurement will enable the investigation of complex protein-membrane interactions in live cells or tissues.

## 1. Introduction

Cargo delivery relies on the tightly regulated membrane fusion between the cargo carriers and target membrane, which is commonly seen in the membrane trafficking during autophagy and neurotransmitter release. Prior to membrane fusion, transport carriers need to dock precisely to the target membrane and recruit the appropriately assembled fusion machinery, a process referred to as membrane tethering. For instance, before neurotransmitter release, membrane tethering facilitates the assembly of soluble N-ethylmaleimide-sensitive factor attachment protein receptor (SNARE) proteins complexes [1,2] to ensure that the synaptic vesicle and presynaptic membrane are in a fusion-ready state. The membranes then fuse to create a small opening until two lipid bilayers of vesicles are merged to form one interconnected structure.

Membrane fusion has been studied at the bulk level via in vitro reconstitution of lipid vesicles, where fused membrane results in changes in optical readout such as the efficiency of Förster (fluorescence) resonance energy transfer (FRET) [3]. However, this bulk strategy cannot probe membrane tethering, which causes no changes in the FRET efficiency. As a result, proteins that specifically regulate member tethering can be misinterpreted as fusion regulators. Functions of the proteins involved in membrane tethering, therefore, remain elusive due to a lack of effective tools to probe the protein-membrane interaction. The recently developed FRET-based single-vesicle assay provides a powerful strategy to study protein functions during

membrane tethering and fusion [4–9]. Because membrane tethering (no FRET) can be effectively differentiated from membrane fusion (high FRET), one can determine the role of the protein of interests on these individual membrane trafficking steps [10]. In this protocol, we introduce a single-vesicle detection method to specifically determine the effect of target proteins on membrane tethering. To demonstrate the effectiveness of this tool, we select two proteins of interests, the cytoplasmic domain of synaptotagmin-1 (C2AB) and α-Synuclein (α-Syn).

The in vitro reconstitution of $Ca^{2+}$-triggered membrane fusion has been widely used to investigate the molecular mechanism underlying membrane trafficking [11]. One of the key molecules in the regulation of $Ca^{2+}$-triggered release of synaptic vesicle fusion is synaptotagmin-1, which contains a C2A domain (binding three calcium ions) and a C2B domain (binding two calcium ions) [12]. After binding to $Ca^{2+}$, C2AB is positively charged so that its affinity for negatively charged lipid molecules increases [13]. Indeed, the fluorometry-based assay [14] has shown that $Ca^{2+}$-associated C2AB was used as molecular glue to mediate the clustering of lipid vesicles [13]. Additionally, the calcium allows C2AB to partially penetrate the lipid membrane to assist in membrane fusion [15]. Thus, C2AB serves as a good candidate for our single-vesicle assay to mechanistically study the $Ca^{2+}$-regulated membrane tethering [16].

The α-Syn is an abundant presynaptic protein associated with synaptic vesicles [17–19]. Overexpression of α-Syn is implicated in neurodegenerative diseases such as Parkinson's disease [20]. The specific role of α-Syn in the regulation of exocytosis and the pathogenesis of

---

Parkinson's disease, however, is unclear [21]. Previous studies suggest that α-Syn binds to the negatively charged phospholipids and interacts with SNARE proteins to regulate the exocytotic pathway in neurons [22,23]. Recently, several research laboratories, including ours, have studied the effect of α-Syn on membrane tethering/docking or fusion via reconstitution of single-vesicle with protein in vitro. Using this method, we found that α-Syn specifically inhibits vesicle docking without interfering with membrane fusion [24]. Choi et al. reported that monomeric α-Syn promotes SNARE-complex formation while α-Syn oligomers impair vesicle association [25]. Note that α-Syn has been previously misinterpreted to reduce membrane fusion based on results from the ensemble lipid-mixing assay [26]. Lou et al. reported that the misfolded α-Syn promoted vesicle docking at low concentrations (< 2.5 μM) but inhibited docking at high concentrations (> 4 μM) [27]. In this protocol, we use our single-vesicle detection method to assess the contribution of α-Syn on membrane tethering.

Single-vesicle detection of membrane fusion promises to reveal the detailed molecular mechanism underlying protein-membrane interactions during membrane trafficking. This strategy, however, has not been widely used. Here, we introduce a protocol that uses total internal reflection fluorescence (TIRF) microscope to measure the protein-membrane interaction at the single-vesicle level. To demonstrate the effectiveness of this technique, we use C2AB and α-Syn, two proteins that are involved in membrane tethering. At the single-vesicle level, no FRET indicates membrane tethering in contrast to membrane fusion, which shows middle to high FRET. Knowledge of protein-induced membrane tethering through the single-vesicle assay will provide quantitative insights into the mechanistic understanding of membrane trafficking.

## 2. Materials and preparatory procedures applied

### 2.1. Reagents

| Name of reagent | Manufacturer | Country |
|---|---|---|
| KOH | Fisher Scientific | USA |
| Methanol | Fisher Scientific | USA |
| Chloroform | Fisher Scientific | USA |
| Acetic acid | Fisher Scientific | USA |
| Sodium bicarbonate | Fisher Scientific | USA |
| HEPES | Fisher Scientific | USA |
| m-PEG, Poly(ethylene glycol) monomethyl ether | Laysan Bio, Inc. | USA |
| Biotin-PEG, Biotinyl-Polyethylene glycol, | Laysan Bio, Inc. | USA |
| NeutrAvidin | Thermo Scientific | USA |
| DOPC, 1,2-dioleoyl-sn-glycero-3-phosphocholine | Polar Lipids, Inc. | USA |
| DOPE, 1,2-dioleoyl-sn-glycero-3-phosphoethanolamine | Polar Lipids, Inc. | USA |
| DOPS, 1,2-dioleoyl-sn-glycero-3-(phospho-L-serine) | Polar Lipids, Inc. | USA |
| Biotin-PE, 1,2-dioleoyl-sn-glycero-3-phosphoethanolamine-N-(biotinyl) | Polar Lipids, Inc. | USA |
| DiI, DiIC18(3) | Life Technologies Corporation | USA |
| DiD, DiIC18(5) | Life Technologies Corporation | USA |
| Amino Silane, (3-(2-Aminoethylamino) propyl) trimethoxysilane | Sigma-Aldrich | USA |
| NaCl | Research Products, Inc. | USA |
| Acetone | VWR | USA |
| Ethanol | Decon Labs, Inc. | USA |
| α-Synuclein | AnaSpec, Inc. | USA |

HEPES buffer: 25 mM HEPES, 100 mM NaCl, pH = 7.4. It should be stored at 4 °C and used within 1 month

### 2.2. Main equipment

| Name of equipment | Manufacturer | Country |
|---|---|---|
| Quartz slides with drilled holes (1 inch × 3 inch, 1 mm thick) | Finkenbeiner Inc. | USA |
| Coverslips (24 mm × 40 mm, rectangular) | VWR | USA |
| Epoxy (5 min) | Devcon | USA |
| Double-sided tape (~100 μm thick) | 3M | USA |
| Forceps | Fisher Scientific | USA |
| Propane torch | Fisher Scientific | USA |
| Glass syringes | Polar Lipids, Inc. | USA |
| Ball container | Sigma-Aldrich | USA |
| Filter membrane (50 nm pores) | Polar Lipids, Inc. | USA |
| 532 nm laser | CrystaLaser LC | USA |
| 640 nm laser | CrystaLaser LC | USA |
| Water-immersion objective lens | Olympus | Japan |
| Dual-band filter | Chroma Technology Corp. | USA |
| Dichroic mirror | Chroma Technology Corp. | USA |
| Electron-multiplying charge-coupled device (EM-CCD) camera | Andor Technology Ltd. | UK |

## 3. Single-vesicle measurement

### 3.1. Prepare PEGylated and biotinylated quartz slides

#### 3.1.1. Clean quartz slides and coverslips

Single-vesicle fluorescence imaging requires an extremely clean surface [28]. To clean quartz slides and coverslips, rinse and sonicate them sequentially in a glass-staining jar with Milli-Q $H_2O$, acetone, 1 M KOH solution, and methanol for 15 min in each step. Slides and coverslips can be reused by first immersing into acetone for more than 24 h in advance, followed by a brief burning with a propane torch (no more than 2 s for coverslips or more than 1 min for slides) to get rid of chemical residues. Chemical residue could increase the fluorescence background and influence the interpretation of single-vesicle measurement. Avoid injury by paying attention to the afterheat and potential fracture of coverslips.

#### 3.1.2. Produce PEGylated and biotinylated surface

3.1.2.1. Crucial step. To eliminate nonspecific adsorption and introduce a binding moiety, passivate the clean surface with m-polyethylene glycol (PEG) and biotin-PEG [29]. A biotinylated surface allows for the immobilization of vesicles via NeutrAvidin. The preparation step consists of two chemical treatments: silanization and biotinylation. Silanization is done by incubation of the clean slides and coverslips in (3-(2-Aminoethylamino) propyl) trimethoxysilane (Amino Silane) solution (100 mL methanol + 5 mL acetic acid + 1 mL Amino Silane) for 10 min, followed by 1 min of sonication. This step is repeated one more time before washing with Milli-Q $H_2O$ and methanol. Each slide or coverslip is then dried by blowing clean nitrogen from the edge. A 100 μL of the reaction solution (120 mg m-PEG + 4 mg biotin-PEG + 700 μL of 0.1 M sodium bicarbonate solution) is then added onto the imaging surface. Each coverslip is carefully placed over each slide and incubated overnight.

3.1.2.2. Note. The Amino Silane solution and the reaction solution should be freshly prepared. The surface of each slide or coverslip should be marked to distinguish the biotinylated side prior to adding the reaction solution containing biotin-PEG. When incubated, the slides and coverslips should be kept in a wet and dark condition to prevent drying or light exposure.

#### 3.1.3. Rinse and storage

After careful disassembly, the slides and coverslips are rinsed with Milli-Q $H_2O$ and dried by blowing clean nitrogen from the edge. Each

set of slide and coverslip is placed into a sealed, 50-mL falcon tube separately and stored at −20 °C for future use.

### 3.2. Assemble the sample chamber

The sample chamber is used for insolating individual reactions. Assemble the sample chamber by sandwiching a double-sided tape between each clean, biotinylated quartz slide and coverslip. Seal the gap between the slide and coverslip at the edge with epoxy [30]. Quartz slides contain holes on both ends so that excess solution can flow out. The sample chamber allows for sequential incubation with different solutions, such as those containing NeutrAvidin, vesicles, and proteins. Immobilized vesicles will appear as diffraction-limited bright spots in the field of view.

#### 3.2.1. Crucial step

Press the coverslips tightly after attaching them to the slides via double-sided tape to prevent leaking between each chamber.

### 3.3. Prepare vesicles

#### 3.3.1. Choose the FRET pair

Ideal dyes for single-vesicle measurement are photo-stable and bright, with minimal intensity fluctuation in the timescale of study. Also, they need to be small enough to incorporate with the vesicles. A good pair of FRET dyes (donor and acceptor) should have appreciable overlap between donor emission and acceptor absorption. The most common dyes pairs are small organic dyes [31], e.g., DiIC18(3) (DiI, donor) and DiIC18(5) (DiD, acceptor). The fluorescence signal of individual vesicles (~50 nm in diameter) stained with DiI or DiD can be detected independently under the excitation of green or red light, respectively. Protein-induced vesicle tethering is quantitatively analyzed by counting the numbers of fluorescent spots at different wavelengths.

#### 3.3.2. Fabricate vesicles

Wash glass syringes and tubes with Milli-Q $H_2O$ and 100% ethanol. Before adding lipid reagents, wash the glass syringe three times with chloroform. The lipid molecules are mixed into the glass tube wrapped with foil contain a small hole on the top. To prepare vesicles with negative charges, the 1,2-dioleoyl-sn-glycero-3-phosphocholine (DOPC), 1,2-dioleoyl-sn-glycero-3-phosphoethanolamine (DOPE), 1,2-dioleoyl-sn-glycero-3-(phospho-L-serine) (DOPS), 1,2-dioleoyl-sn-glycero-3-phosphoethanolamine-N-(biotinyl) (Biotin-PE) and fluorescent dye (DiI or DiD in ethanol) are included in the composition required. The lipid composition of PS-free vesicles (without DOPS) is similar to that of vesicles with 12% negatively charged DOPS except for replacing 12% DOPS with DOPC.

Mix each lipid component in a glass test tube using glass syringe as follows (Table 1).

##### 3.3.2.1. Crucial step. Vacuum test tubes in a ball container, carefully rotate the tubes every 30 min until the organic solvent is evaporated and a thin film is formed at the bottom of tubes. Add HEPES buffer into the tube to resuspend the lipid film. Transfer the lipid film solution to a fresh test tube and sonicate for 3 min. Freeze-thaw at least 5~6 times by

**Table 1**
Formula for the preparation of DiI and DiD vesicles (12% PS).

|  | DiI vesicles (mol%) | DiD vesicles (mol%) |
| --- | --- | --- |
| DOPC | 65.8 | 66 |
| DOPE | 20 | 20 |
| DOPS | 12 | 12 |
| DiI | 2 | — |
| DiD | — | 2 |
| Biotin-PE | 0.2 | — |

alternating submerging in liquid nitrogen and then warming at 60 °C. Store the solution in a −80 °C freezer for future use. Before use, filter the solution through a membrane with 50 nm pores by extrusion to obtain monodispersed vesicles.

### 3.4. Image the single vesicles with TIRF microscope

A homemade TIRF microscope is used to observe the protein-induced membrane tethering of single-vesicles. The microscope consists of five modules: light source, optical system, imaging platform, electron-multiplying charge-coupled device (EMCCD) detector, and the data acquisition program (Fig. 1b).

The light source contains two solid-state lasers at 532 nm (green) and 633 nm (red). Their intensity can be controlled with neutral density filters. We use 532 nm light to excite the donor DiI (donor)-labeled vesicles and 633 nm light to excite the DiD (acceptor)-labeled vesicles. The laser beams pass from the light source through the prism and refractive index–matching oil to be internally reflected at the quartz-water interface. Fluorophores within single-vesicles are excited by lasers at the appropriate excitation wavelength (Fig. 1a), and the fluorescence signals are collected using a water immersion objective fixed on an inverted fluorescence microscope. Donor and acceptor fluorescence emission is then split using a dichroic mirror. The fluorescence signal is detected with an EMCCD with high quantum efficiency, fast vertical shift speeds, low effective readout noise, and multiplication noise. Both donor (DiI) and acceptor (DiD) emission signals are collected simultaneously by the EMCCD camera. Fluorescence signals can be recorded and analyzed in real time using the custom software obtained from Dr. Taekjip Ha's group at the Johns Hopkins University.

## 4. Measure protein-induced membrane tethering at the single-vesicle level

### 4.1. Single-vesicle measurement of α-Syn-induced membrane tethering

Add 50 μL of 0.1 mg/mL NeutrAvidin into the sample channel and incubate for 5 min. Inject the DiI vesicles solution into the sample chamber and incubate for 30 min. After buffer change, inject the α-Syn solution into the sample chamber and incubate for 30 min. The protein should be bound to the surface of immobilized DiI vesicles (Fig. 2). Rinse out unbound α-Syn with HEPES buffer, inject the DiD vesicles solution and incubate for 30 min. Before taking images with the TIRF microscope, rinse with HEPES buffer three times to remove uncombined DiD vesicles.

#### 4.1.1. Note

During injection, ensure that no bubbles form in the sample chamber to avoid vesicles breakup. Run all samples and controls on the same slide and under identical conditions. Use the same laser intensity to record images from different sample channels.

#### 4.1.2. Crucial step

The Biotin-PE moiety on the DiI vesicles will rapidly immobilize the vesicle on the surface of NeutrAvidin-labeled quartz slides. Check the field of view under the microscope to make sure DiI vesicles are homogeneously distributed before adding proteins or floating DiD-containing vesicles (Fig. 2), which is crucial for measuring the membrane tethering of DiD vesicles accurately. The channel containing all solutions except α-Syn should be set up in parallel. The vesicles sample with different lipid components and with different surface charges could also be compared by following the above procedure. Replicates should be measured on the same slides to minimize batch-to-batch variation.

Because DiD vesicles only tether on the α-Syn-bound DiI vesicles, the capacity of α-Syn-induced membrane tethering should be proportional to the ratio of combined DiD/DiI vesicles over unbound DiI
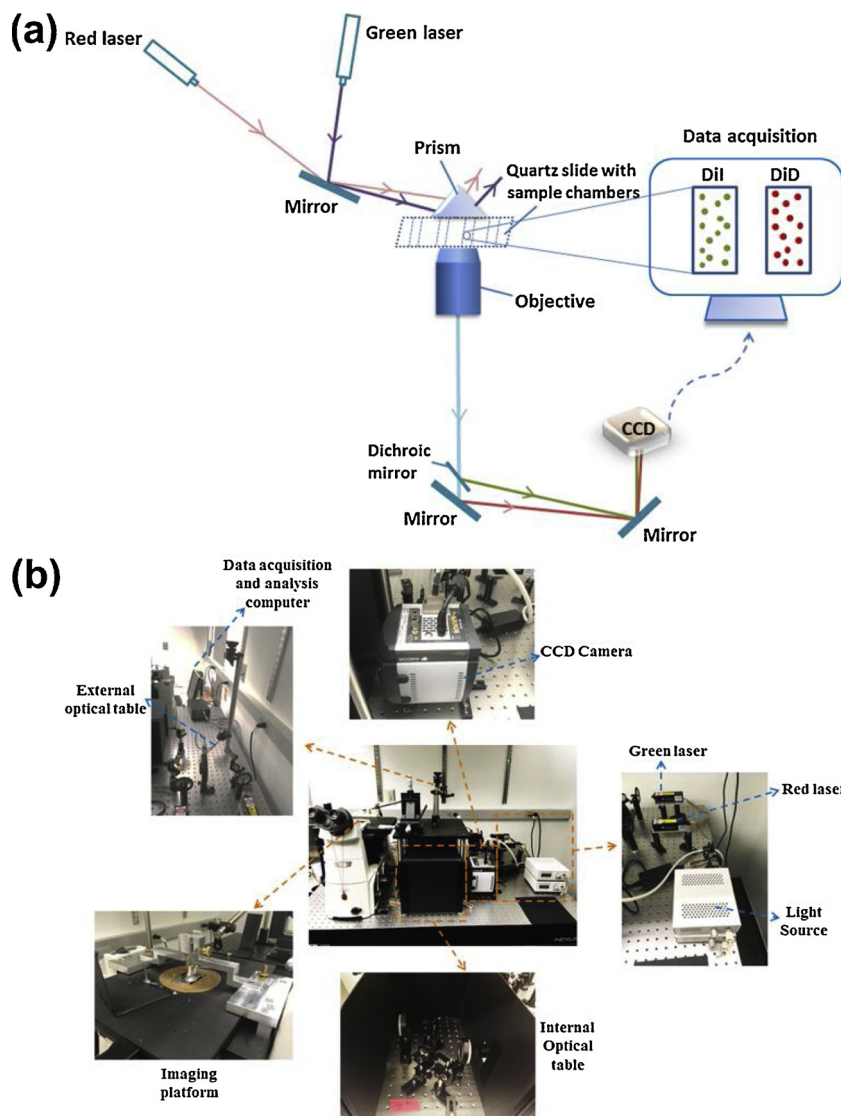
**Fig. 1.** (a) Schematic diagram of the imaging and detection system; (b) Photographs of different parts of the system.
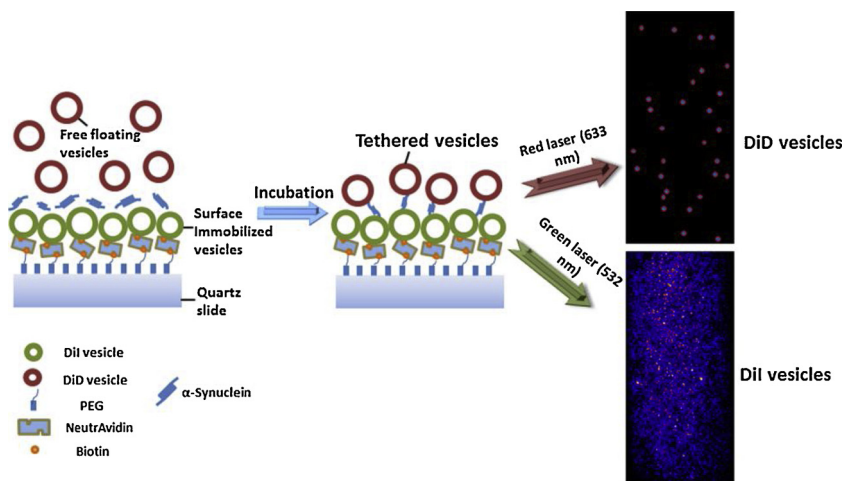


**Fig. 2.** Schematic illustration of single-vesicle measurement of α-Syn induced membrane tethering. The image size is 25 × 50 μm.
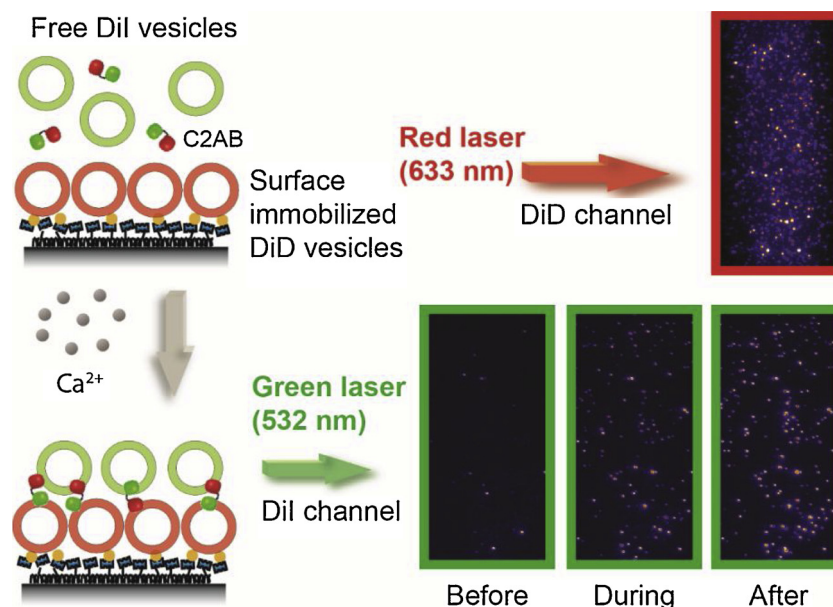
**Fig. 3.** Schematic illustration and representative experimental results $Ca^{2+}$-mediated C2AB-induced membrane tethering measured at the single-vesicle level. The image size is $25 \times 50 \, \mu m$.

vesicles in a field of view. Note that DiI vesicles were prepared to form a homogeneous layer on the surface, this ratio is therefore proportional to the number of DiD vesicles in a field of view. During data acquisition, more than 10 random field of views should be imaged and analyzed for each sample. Results are reported as mean ± standard deviations from more than 10 images. One-way Analysis of Variance (ANOVA) with the Turkey Test is used to determine the statistical significance among different groups. The difference is considered extremely statistically significant when the p-value is less than 0.001 (***).

### 4.1.3. Crucial step

The extent of vesicle-tethering is calculated as the ratio of the number of fluorescent spots in the acceptor channel over the number of spots in the donor channel. The analysis data scale for the fluorescent intensity based on no α-Syn case should be set as the same when analyzing the parallel tests.

### 4.2. Single-vesicle measurement of C2AB-induced membrane tethering triggered by calcium

The single-vesicle measurement of membrane tethering induced by C2AB is similar to that induced by α-Syn with slightly different protein concentrations and the order of vesicles addition. The donor (DiI, green)-labeled vesicles are free-floating in solution, whereas the acceptor (DiD, red)-labeled vesicles are immobilized on the surface (Fig. 3a). To prepare the surface immobilized DiD-labeled vesicles, add 20 μL of 0.1 mg/mL NeutrAvidin into the sample channel and incubate for 5 min. Inject the DiD vesicle solution into the sample chamber and incubate for 40 min. Rinse excess DiD vesicles with HEPES buffer at least 4 times (100 μL each time). The solution containing 1 μM DiI vesicles and 1 μM C2AB is then injected into the sample chamber. Supply the chamber immediately with a solution containing the relevant ions with 3 injections (100 μL per injection). Upon exposure to specific ions (e.g., $Ca^{2+}$, $Zn^{2+}$), C2AB molecules change conformation and form a linkage between DiD and DiI vesicles (Fig. 3b). Rinse out free DiI vesicles with HEPES buffer three times before data acquisition.

## 5. Expected results

Membrane fusion could happen together with or immediately after

the tethering, which reduces the apparent extent of membrane tethering. To exclude the effect of membrane fusion on the tethering measurement, one should ensure that the FRET efficiency does not change between each pair of vesicles after washing away free-floating DiD vesicles. The no FRET value (shown in Fig. 4b) indicates the two fluorophores between the vesicles are separated beyond their Förster distance [32]. Since membrane fusion may give rise to higher FRET value, only the DiD vesicles with a low FRET value are calculated as undergoing membrane tethering.

Figs. 4 and 5 show α-Syn and $Ca^{2+}$/C2AB-mediated membrane tethering between DiD vesicles and DiI vesicles, respectively. To minimize the non-specific binding of DiD vesicles, the surface was covered by a layer of DiI vesicles at a high density before any proteins were added. The number of tethered DiD vesicles significantly increased after α-Syn was added, indicating its positive role in regulating membrane tethering (Fig. 4c–d). Similarly, assisted by $Ca^{2+}$ (or $Zn^{2+}$), the addition of C2AB triggers membrane tethering, as evidenced by the increased number of tethered DiD vesicles. We speculate that $Ca^{2+}$ (or $Zn^{2+}$) can facilitate C2AB to partially penetrate the lipid membrane, which assists the binding between DiI vesicles and DiD vesicles. The efficiency of C2AB-mediated membrane tethering increases as the concentration of $Ca^{2+}$ or $Zn^{2+}$ increases. Other ions including $Mg^{2+}$, $Fe^{2+}$, and $Cu^{2+}$, do not have a significant effect on the C2AB-mediated membrane tethering, which makes sense because C2A and C2B domains do not bind to those ions (Fig. 5).

## 6. Future prospects

TIRF microscope and home-developed data acquisition and analysis software allow us for single-vesicle measurement of protein-induced membrane tethering. This strategy enables the investigation of proteins to membrane tethering in a quantitative manner. The system can be generalized to study more complex tethering behavior by including more dyes. Also, one can conjugate fluorophores on specific proteins to track them directly and study their roles on membrane tethering in real time. Furthermore, this strategy can be modified to measure membrane tethering in live cells with emerging techniques such as the high-resolution technique of two-dimension imaging, fluorescence correlation spectroscopy and related technologies that enable point detection in three-dimension space [33].
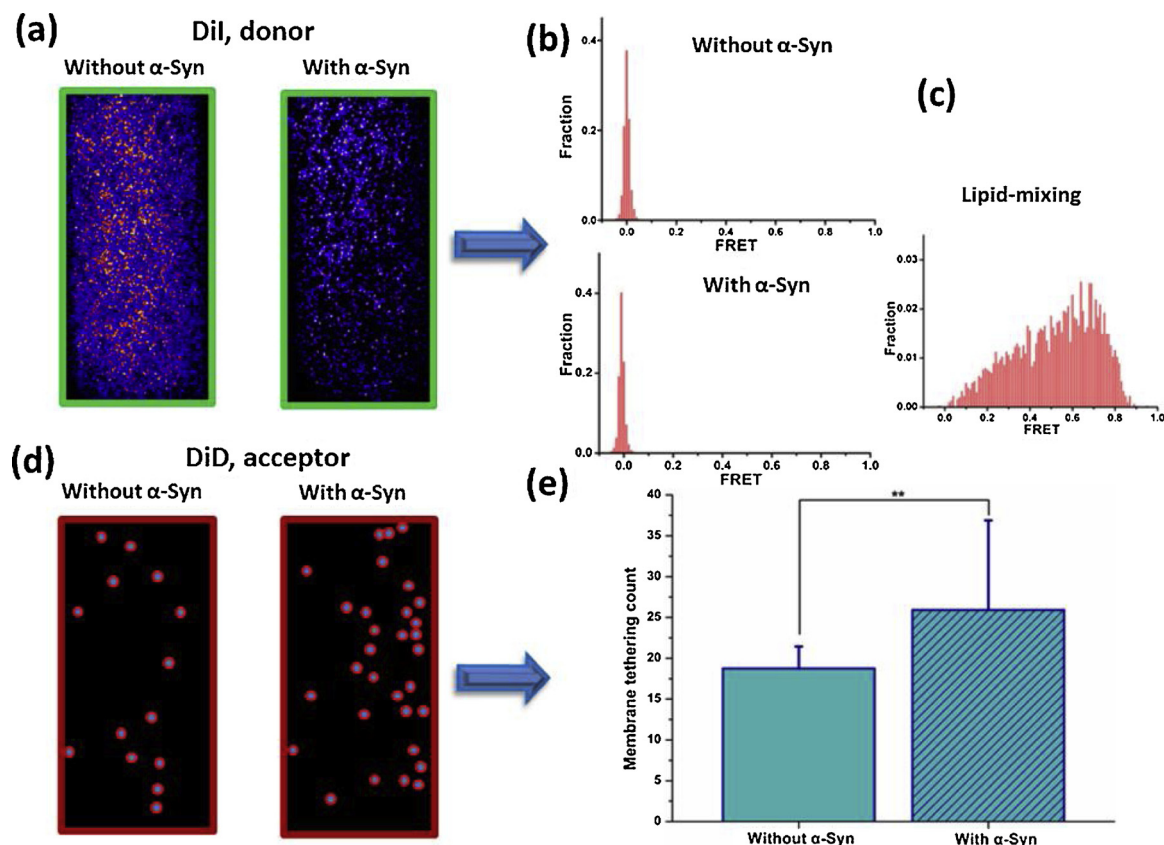
**Fig. 4.** (a) The images of immobilized DiI vesicles with and without induction of α-Syn under excitation of the green laser (532 nm). (b) The FRET histograms of fluorescence spots in the channels with and without induction of α-Syn. (c) The FRET histogram of SNARE-mediated lipid mixing. (d) The images of tethered DiD vesicles with and without induction of α-Syn under excitation of the red laser (633 nm). (e) The corresponding statistics results of membrane tethering count based on the images of tethered DiD vesicles (** p < 0.01). The image size is 25 × 50 μm (For interpretation of the references to colour in this figure legend, the reader is referred to the web version of this article).



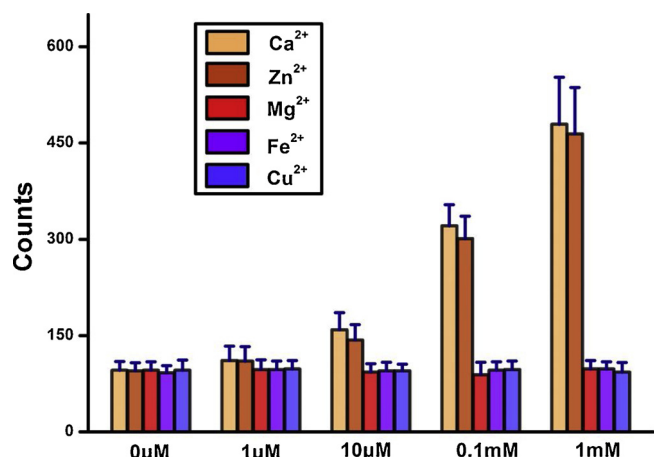**Fig. 5.** Dose-dependent quantification of C2AB-induced membrane tethering treated with the different ion. $Ca^{2+}$ and $Zn^{2+}$ play a more significant role in membrane tethering than other ions.

## Competing interests

The authors declare no potential conflicts of interest with respect to authorship and publication of this article.

## Acknowledgments

## References

[1] Y. Wang, L. Li, C. Hou, Y. Lai, J. Long, J. Liu, Q. Zhong, J. Diao, SNARE-mediated membrane fusion in autophagy, Semin. Cell Dev. Biol. 60 (2016) 97–104.
[2] A.T. Brunger, D.J. Cipriano, J. Diao, Towards reconstitution of membrane fusion mediated by SNAREs and other synaptic proteins, Crit. Rev. Biochem. Mol. Biol. 50 (2015) 231–241.
[3] D.K. Struck, D. Hoekstra, R.E. Pagano, Use of resonance energy transfer to monitor membrane fusion, Biochemistry 20 (1981) 4093–4099.
[4] J. Diao, L. Li, Y. Lai, Q. Zhong, In vitro reconstitution of autophagosome-lysosome fusion, Methods Enzymol. 587 (2017) 365–376.
[5] J. Diao, Z.L. Su, Y. Ishitsuka, B. Lu, K.S. Lee, Y. Lai, Y.K. Shin, T. Ha, A single-vesicle content mixing assay for SNARE-mediated membrane fusion, Nat. Commun. 1 (2010) 54.
[6] J.J. Diao, M.L. Zhao, Y.X. Zhang, M. Kyoung, A.T. Brunger, Studying protein-re-constituted proteoliposome fusion with content indicators in vitro, Bioessays 35 (2013) 658–665.
[7] M. Kyoung, A. Srivastava, Y.X. Zhang, J.J. Diao, M. Vrljic, P. Grob, E. Nogales, S. Chu, A.T. Brunger, In vitro system capable of differentiating fast Ca(2+)-trig-gered content mixing from lipid exchange for mechanistic studies of neuro-transmitter release, Proc. Natl. Acad. Sci. U. S. A. 108 (2011) E304–E313.
[8] M.J. Kyoung, Y.X. Zhang, J.J. Diao, S. Chu, A.T. Brunger, Studying calcium-trig-gered vesicle fusion in a single vesicle-vesicle content and lipid-mixing system, Nat. Protoc. 8 (2013) 1–16.
[9] Z. Tian, J. Gong, M. Crowe, M. Lei, D. Li, B. Ji, J. Diao, Biochemical studies of membrane fusion at the single-particle level, Prog. Lipid Res. 73 (2019) 92–100.
[10] J. Diao, Y. Ishitsuka, W.R. Bae, Single-molecule FRET study of SNARE-mediated membrane fusion, Biosci. Rep. 31 (2011) 457–463.

[11] W.C. Tucker, T. Weber, E.R. Chapman, Reconstitution of Ca2 + -regulated membrane fusion by synaptotagmin and SNAREs, Science 304 (2004) 435–438.

[12] J. Rizo, X.C. Chen, D. Arac, Unraveling the mechanisms of synaptotagmin and SNARE function in neurotransmitter release, Trends Cell Biol. 16 (2006) 339–350.

[13] J. Diao, T.Y. Yoon, Z. Su, Y.K. Shin, T. Ha, C2AB: a molecular glue for lipid vesicles with a negatively charged surface, Langmuir 25 (2009) 7177–7180.

[14] Q. Wang, X. Zhai, M. Crowe, L. Gou, Y. Li, D. Li, L. Zhang, J. Diao, B. Ji, Heterogeneous oxidization of graphene nanosheets damages membrane, Sci. China Ser. G Phys. Mech. Astron. 62 (2018) 64611.

[15] S. Martens, M.M. Kozlov, H.T. McMahon, How synaptotagmin promotes membrane fusion, Science 316 (2007) 1205–1208.

[16] J. Diao, P. Grob, D.J. Cipriano, M. Kyoung, Y. Zhang, S. Shah, A. Nguyen, M. Padolina, A. Srivastava, M. Vrljic, A. Shah, E. Nogales, S. Chu, A.T. Brunger, Synaptic proteins promote calcium-triggered fast transition from point contact to full fusion, eLife 1 (2012) e00109.

[17] B. Bu, X. Tong, D. Li, Y. Hu, W. He, C. Zhao, R. Hu, X. Li, Y. Shao, C. Liu, Q. Zhao, B. Ji, J. Diao, N-terminal acetylation preserves alpha-synuclein from oligomerization by blocking intermolecular hydrogen bonds, ACS Chem. Neurosci. 8 (2017) 2145–2151.

[18] R. Hu, J. Diao, J. Li, Z. Tang, X. Li, J. Leitz, J. Long, J. Liu, D. Yu, Q. Zhao, Intrinsic and membrane-facilitated alpha-synuclein oligomerization revealed by label-free detection through solid-state nanopores, Sci. Rep. 6 (2016) 20776.

[19] J. Burre, S. Vivona, J. Diao, M. Sharma, A.T. Brunger, T.C. Sudhof, Properties of native brain alpha-synuclein, Nature 498 (2013) E4–E6 discussion E6-7.

[20] M. Goedert, Alpha-synuclein and neurodegenerative diseases, Nat. Rev. Neurosci. 2 (2001) 492–501.

[21] C. Wang, C. Zhao, D. Li, Z. Tian, Y. Lai, J. Diao, C. Liu, Versatile structures of alpha-synuclein, Front. Mol. Neurosci. 9 (2016) 48.

[22] J. Diao, J. Burre, S. Vivona, D.J. Cipriano, M. Sharma, M. Kyoung, T.C. Sudhof, A.T. Brunger, Native alpha-synuclein induces clustering of synaptic-vesicle mimics via binding to phospholipids and synaptobrevin-2/VAMP2, Elife 2 (2013) e00592.

[23] J. Burre, M. Sharma, T. Tsetsenis, V. Buchman, M.R. Etherton, T.C. Sudhof, Alpha-synuclein promotes SNARE-Complex assembly in vivo and in vitro, Science 329 (2010) 1663–1667.

[24] Y. Lai, S. Kim, J. Varkey, X. Lou, J.K. Song, J. Diao, R. Langen, Y.K. Shin, Nonaggregated alpha-synuclein influences SNARE-Dependent vesicle docking via membrane binding, Biochemistry 53 (2014) 3889–3896.

[25] B.K. Choi, M.G. Choi, J.Y. Kim, Y. Yang, Y. Lai, D.H. Kweon, N.K. Lee, Y.K. Shin, Large alpha-synuclein oligomers inhibit neuronal SNARE-mediated vesicle docking, Proc. Natl. Acad. Sci. U. S. A. 110 (2013) 4087–4092.

[26] D.C. DeWitt, E. Rhoades, Alpha-synuclein can inhibit SNARE-Mediated vesicle fusion through direct interactions with lipid bilayers, Biochemistry 52 (2013) 2385–2387.

[27] X. Lou, J. Kim, B.J. Hawk, Y.K. Shin, Alpha-Synuclein may cross-bridge v-SNARE and acidic phospholipids to facilitate SNARE-dependent vesicle docking, Biochem. J. 474 (2017) 2039–2049.

[28] Y. Hu, Z. Tian, J. Diao, Single-molecule fluorescence measurement of SNARE-Mediated vesicle fusion, Methods Mol. Biol. (Clifton, N.J.) 1860 (2019) 335–344.

[29] S.D. Chandradoss, A.C. Haagsma, Y.K. Lee, J.H. Hwang, J.M. Nam, C. Joo, Surface passivation for single-molecule protein studies, J. Vis. Exp. (2014).

[30] J. Diao, Y. Ishitsuka, H. Lee, C. Joo, Z. Su, S. Syed, Y.K. Shin, T.Y. Yoon, T. Ha, A single vesicle-vesicle fusion assay for in vitro studies of SNAREs and accessory proteins, Nat. Protoc. 7 (2012) 921–934.

[31] A.N. Kapanidis, S. Weiss, Fluorescent probes and bioconjugation chemistries for single-molecule fluorescence analysis of biomolecules, J. Chem. Phys. 117 (2002) 10953–10964.

[32] C. Joo, T. Ha, Single-molecule FRET with total internal reflection microscopy, Cold Spring Harb. Protoc. 2012 (2012).

[33] Y. Sako, M. Hiroshima, C.G. Pack, K. Okamoto, K. Hibino, A. Yamamoto, Live cell single-molecule detection in systems biology, Wiley Interdiscip. Rev. Syst. Biol. Med. 4 (2012) 183–192.